Journal of Photochemistry and Photobiology A: Chemistry 229 (2012) 11–19

Contents lists available at SciVerse ScienceDirect

Journal of Photochemistry and Photobiology A: Chemistry

journal homepage: www.elsevier.com/locate/jphotochem

Influence of adsorption on the photocatalytic properties of TiO_2/AC composite materials in the acetone and cyclohexane vapor photooxidation reactions

D.S. Selishchev, P.A. Kolinko, D.V. Kozlov*

Boreskov Institute of Catalysis, Novosibirsk 630090, Russian Federation

ARTICLE INFO

Article history:
Received 14 June 2011
Received in revised form 5 December 2011
Accepted 10 December 2011
Available online 19 December 2011

Keywords:
Gas-phase photocatalysis
Adsorption
Titanium dioxide
Activated carbon

ABSTRACT

A series of TiO_2/AC composite photocatalysts with various TiO_2 contents was prepared by thermal hydrolysis method of a $TiOSO_4$ water solution in the presence of activated carbon particles. XRD, SEM and BET methods revealed that in all cases deposited TiO_2 is an anatase with ~170 m^2/g specific surface area. All samples were tested in gaseous acetone and cyclohexane vapor photocatalytic oxidation in static and continuous flow reactors. Complete photocatalytic mineralization of both model pollutants without formation of gaseous intermediates was observed. Only TiO_2/AC catalysts with TiO_2 content higher than 50% demonstrated good photocatalytic activity. The same amounts of individual TiO_2 and AC powders as in the case of 70%-TiO_2/AC composite photocatalyst were placed separately in the static reactor and kinetic curves of the cyclohexane photocatalytic oxidation were compared for both cases. When TiO_2 and AC were used separately complete mineralization of cyclohexane was not observed even after 4 h of the PCO. Whereas in the case of 70%-TiO_2/AC sample expected CO_2 level was almost achieved after 120 min. The most likely reason of this difference is the absence of reagents and intermediates surface transfer between separated individual TiO_2 and AC powders.

L.-H. kinetic model was used to describe experimental data in the flow reactor. Obtained results demonstrated that effective adsorption constants for TiO_2/AC photocatalysts were about 2 times higher than for pure TiO_2. Model of TiO_2/AC composite photocatalyst with increased photocatalytic and adsorption properties was suggested.

1. Introduction

Well-known methods for water and air purification are based on the usage of certain types of adsorbents. The most popular adsorbent is activated carbon (AC) due to its high pore volume and surface area and high adsorption capacity [1]. Main drawback of pollutants removal with adsorbent is the decrease of purification efficiency with time and importance of regular regeneration. There also exists a problem of further utilization of accumulated pollutants.

Heterogeneous photocatalytic oxidation (PCO) is promising method to remove volatile organic compounds (VOCs) from indoor air especially at low concentrations, because it allows a lot of pollutants to be oxidized with formation of CO_2 and H_2O as final products [2,3]. Most of researches are focused on the application of TiO_2 as photocatalyst due to its high activity [4–6]. Titanium dioxide allows many type of organic compound to be decomposed effectively both in air and in water [7–9]. However, there are some limitations of TiO_2-mediated photocatalytic oxidation. The first drawback is the low adsorption capacity of TiO_2 and insufficient PCO rate. As a result it is usually required a long time to mineralize organic admixtures completely. The second drawback is a formation of intermediates, which could cause photocatalyst deactivation, for example, in the case of aromatic and heteroatom containing organic compounds PCO [10,11]. Sometimes intermediates could be more harmful than starting pollutant [12], and in this case the PCO could become the source of even higher air or water pollution.

Photocatalytic process could be considered as substrate adsorption on the catalyst surface and subsequent oxidation by active species forming under UV irradiation. On this basis it is possible to modify photocatalysts to increase efficiency of photocatalytic oxidation process at every step: adsorption and oxidation. Kinetic constant could be increased, for example, by noble metals depositions on the catalysts surface [13]. In this case metal particles accumulate electrons improving charge separation and reducing electron–hole recombination rate giving the overall enhancement of photoreactions efficiency. Adsorption constant could be increased by H_2SO_4 treatment of the TiO_2 surface [13].

An alternative way of improving photocatalyst adsorption ability is addition of adsorbent in the photocatalytic system or making TiO_2/adsorbent composite system, in which TiO_2 would be deposited on adsorbent surface. In the first case photocatalyst

* Corresponding author. Tel.: +7 383 3331617; fax: +7 383 3331617.
E-mail address: kdv@catalysis.ru (D.V. Kozlov).

1010-6030/$ – see front matter © 2011 Elsevier B.V. All rights reserved.
doi:10.1016/j.jphotochem.2011.12.006

and adsorbent are used separately [14]. Shiraishi et al. [15] used a photocatalytic reactor combined with a continuous adsorption and desorption apparatus for treatment of gaseous formaldehyde in a small chamber. Other researchers [16] used aqueous suspended mixture of TiO_2 and AC for the photocatalytic degradation of phenol. They revealed that the apparent first-order rate constants were higher for mixed TiO_2 + AC system than for TiO_2 alone.

Earlier we reported the computer simulation study and demonstrated that in the case of separate adsorbent and photocatalyst usage adsorbent works as a buffer [17]. On the other hand the use of supported TiO_2/adsorbent photocatalyst could be more beneficial due to reversible surface transfer of reagents and intermediates from catalyst to adsorbent surface. In this case the gaseous intermediates concentration as well as the effective time of substrate removal could be decreased [17]. Supported TiO_2/adsorbent photocatalysts have been extensively investigated in the recent time. A number of materials were used as a TiO_2 support: glass [18], organic and inorganic fibers [19], activated carbon [20], SiO_2 [18] and Al_2O_3 [21]. Torimoto and co-workers [22] demonstrated that the rate of CO_2 accumulation for propyzamide oxidation over 70%-TiO_2/adsorbent photocatalysts was reduced in the adsorbent sequence AC–SiO_2–mordenite–pure TiO_2. It correlated with amount of adsorbed substrate. Takeda and co-workers [23] reported that the highest formation rate of final product – CO_2 in the photodecomposition of gaseous propionaldehyde was observed for a TiO_2/adsorbent photocatalysts with medium adsorption constant.

Many researchers investigated carbon materials, and AC in particular, in combination with TiO_2. A lot of methods were applied to prepare photocatalytically active TiO_2/AC samples: aggregation into solution [24], sol–gel [25], hydrothermal synthesis [26], CVD [27]. Some good reviews regarding preparation routes and their effects on photocatalytic activity of TiO_2/AC have been published recently [28,29]. Most investigations are devoted to photocatalytic oxidation of pollutants over TiO_2/AC in water solutions [26,27,30]. Enhanced photocatalytic activity of TiO_2/AC in comparison to TiO_2 alone (synergism) are often explained by adsorption of substrate on AC surface followed by surface transfer to photocatalytically active TiO_2. This conclusion is often based on the analysis of substrate removal kinetic curve only. According to our opinion such approach is not sufficient because faster substrate removal could be explained by adsorption whereas photocatalytic activity of composite TiO_2/AC system could be decreased. In this way analysis of products accumulation kinetic curves should be done also.

A quantity of papers about gas-phase oxidation with mixed TiO_2/adsorbent photocatalysts is much smaller. Kuo et al. [31] used TiO_2(P25)/AC photocatalyst in a fluidized bed photoreactor for toluene oxidation at 200–1000 ppm toluene concentration in flow reactor. They revealed that TiO_2/AC catalysts had high adsorption capability and steady-state toluene conversion was about 3 times higher with TiO_2/AC photocatalyst than with pure TiO_2. In some conditions toluene concentration could be reduced to the maximum contaminant level (about 100 ppm) and kept in this stage for at least 11 h. Other researchers [32] immobilized TiO_2 on an activated carbon (TiO_2/AC) filter installed in a commercial air cleaner and tested it in the PCO of NO and toluene removal at ppb level. Bouazza and co-workers [33] prepared pellets of TiO_2 P25 and pellets of 70%-TiO_2/AC and used them in photocatalytic oxidation of propene and benzene in dry and humidified conditions. In humidified air the agglomerated TiO_2/AC photocatalyst was the most active for benzene PCO. On the other hand Torimoto et al. [34] reported that in gaseous dichloromethane oxidation the photocatalytic activity of chemically prepared 80%-TiO_2/AC catalyst was lower than for unmodified TiO_2.

To summarize it could be concluded that presence of AC in photocatalysts composition could be positive or negative for different type of organic compounds and this effect depends on the nature of interaction between substrate and support. Investigations of pollutant photooxidation in gas phase have received insufficient researcher's attention. In present work we compared kinetics of gaseous substrates photocatalytic oxidation in static and flow reactors for TiO_2/AC catalysts since this question still remained without attention. Acetone and cyclohexane were chosen as polar and nonpolar model substrates and kinetics of their PCO was investigated using different TiO_2/AC photocatalysts prepared by thermal hydrolysis method.

2. Materials and methods

2.1. Reagents

Activated carbon powder (SORBENT Inc., Russia) was chosen as a porous support for TiO_2 deposition. Before synthesis it was washed out thoroughly by distilled water. The other reagents were purity grade and used for synthesis of catalysts and oxidation experiments as purchased: sulfuric acid (H_2SO_4, 93.5–95.6%, PKF ANT Inc., Russia), titanyl sulfate ($TiOSO_4{\cdot}2H_2O$, >98%, VEKTON Inc., Russia), acetone (CH_3COCH_3, >99.8%, MOSREAKTIV Inc., Russia), cyclohexane (C_6H_{12}, >99%, PIRIMIDIN Inc., Ukraine).

Titanyl sulfate water solution used for thermal hydrolysis synthesis was approximately 10 wt.% concentration and was prepared by dissolution of 50–55 g of $TiOSO_4{\cdot}2H_2O$ in 450 ml of distilled water during 24 h at constant mixing. Finally, small amount of the undissolved $TiOSO_4$ was separated by centrifugation. As prepared solution was then stabilized by addition of H_2SO_4 to adjust its concentration to about 0.1 M value. Final $TiOSO_4$ solution was kept in cold.

2.2. Catalysts preparation

Brief description of thermal hydrolysis synthesis is shown in Fig. 1. The main varying parameter was the TiO_2 content in the sample. To prepare 1 g of TiO_2/AC sample with X wt.% TiO_2 content $(1-(X/100))$ g of AC were suspended into the $V=(X/8C)$ ml of $TiOSO_4$ water solution with concentration C (mol/l). Samples in this series were marked as X-TC where X was the TiO_2 content (wt.%). TiO_2 sample (without AC) synthesized by thermal hydrolysis was marked as s-TiO_2.

2.3. Characterization of catalysts

TiO_2 content in X-TC series was measured using the X-ray fluorescence spectrometer VRA-30 with chromic anode. The morphology of samples was studied by scanning electron microscopy (SEM) using the LEO-430 spectrometer (Carl Zeiss). N_2 adsorption isotherms were measured at 77 K using a Micromeritics ASAP 2020 instrument. The specific surface area was calculated by the BET method. For pore volume characterization was used single point adsorption total pore volume at $(P/P_0)\sim 1$. The crystal phase identification was carried out by the X-ray powder diffraction with a X'tra (Thermo) diffractometer using CuK_α radiation and scanning in the 2θ range of 15–85°. The (2 0 0) plane diffraction peak for anatase ($2\theta = 48.09°$) was used to calculate TiO_2 crystallite size on the assumption of spherical shape. UV–vis diffuse reflectance spectra were measured using Lambda 35 spectrophotometer (Perkin Elmer) equipped a diffuse reflectance accessory with reference to MgO powder.

2.4. Kinetic measurements

In the present work two types of reactor were used for kinetic experiments.

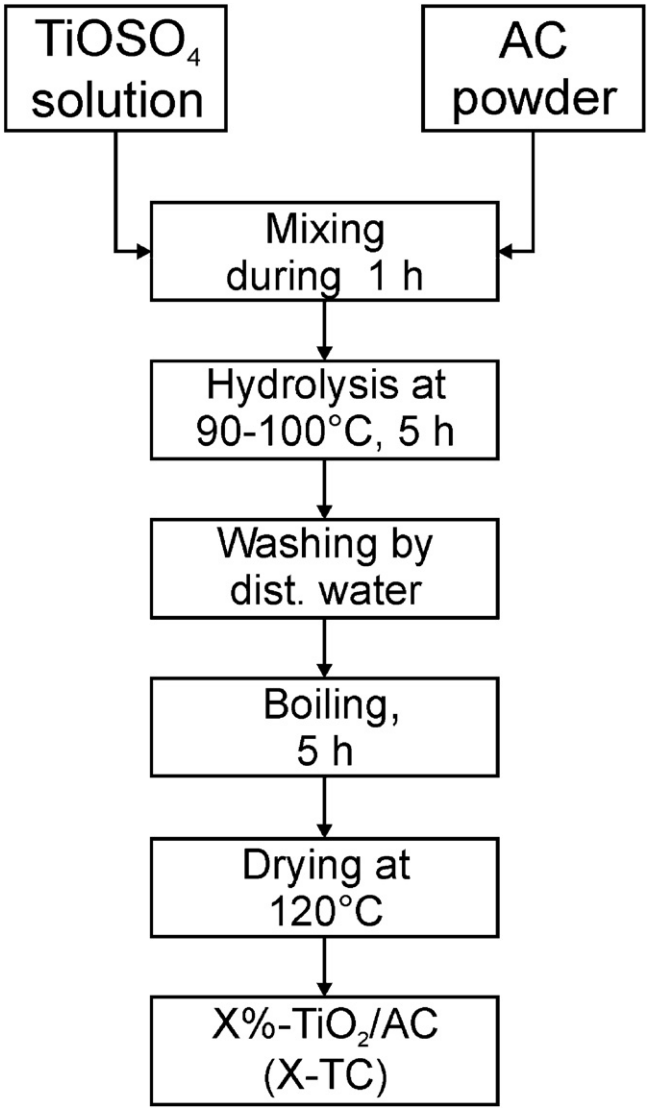

Fig. 1. Brief description of TiO_2/AC photocatalysts preparation by $TiOSO_4$ thermal hydrolysis.

Static reactor (Fig. 2) was used for acetone and cyclohexane vapor PCO kinetic measurements. This reactor was installed in the cell compartment of Nicolet 380 (Thermo) FTIR spectrometer.

Samples were uniformly deposited onto the glass support so that illuminated area was about 3.1 cm^2 for acetone oxidation and 7 cm^2 for cyclohexane oxidation. Photocatalyst density was 1 mg/cm^2 to provide complete light absorption. Before the beginning of every experiment photocatalyst samples were irradiated with UV light during 3–4 h in order to completely oxidize some previously adsorbed surface species. Then a certain amount of liquid acetone (0.4 μl) or cyclohexane (0.8 μl) was injected and evaporated for 30 min until adsorption–desorption equilibrium was established. Finally the illumination was turned on and gas-phase IR spectra were taken periodically.

Steady-state values of cyclohexane PCO rate were measured *in a flow-circulating reactor* (Fig. 3). The cyclohexane PCO was studied at substrate concentration range 0–30 μmol/l. Other operational parameters were: temperature – 40 °C, relative humidity (RH) – 46 ± 2%, volumetric flow rate (U) – 28 cm^3/min, Phillips 9 W 365 nm UV-A light source, irradiated area of the sample ~ 7 cm^2, sample density – 1 mg/cm^2.

The CO_2 and cyclohexane concentrations were measured using gas cell (Fig. 3(7)) installed in the cell compartment of Nicolet 380 (Thermo) FTIR spectrometer. The PCO rate was calculated according to the following formula: $W_{CO_2} = \Delta C_{CO_2} \cdot U$, where ΔC_{CO_2} is the difference of CO_2 concentrations in the outlet and inlet of the flow reactor, U is volumetric flow rate.

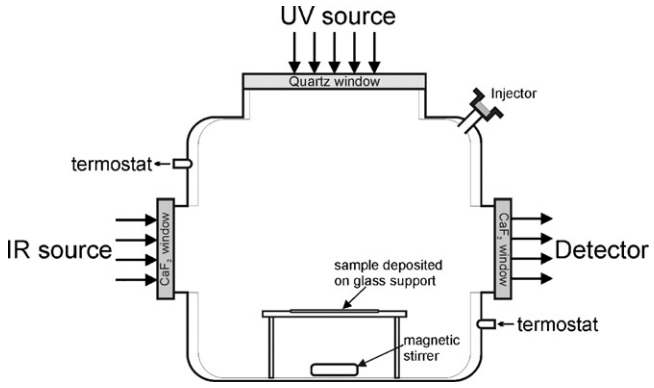

Fig. 2. The static reactor for kinetic measurements. Experimental conditions: reactor volume 300 cm^3; temperature 25 °C; optical path length 10 cm; irradiation by light of 1000 W high pressure Hg lamp DRSH 1000 (Russia) which was passed through a BS-4 300 nm cutoff filter, UV light intensity 13 mW/cm^2.

Table 1
TiO_2 content and textural properties of TC series samples.

Sample	TiO_2 content (wt.%)	BET surface area, A (m^2/g)	Single point total pore volume, V (cm^3/g)
AC	–	825	0.54
s-TiO_2	100	167	0.20
80-TC	78.0	317	0.29
70-TC	67.0	389	0.34
50-TC	50.1	510	0.35
30-TC	31.9	639	0.40
20-TC	21.0	696	0.42

3. Results and discussion

3.1. Characteristics of synthesized photocatalysts

Five samples of TC series were synthesized with TiO_2 content 20, 30, 50, 70 and 80 wt.%. Results of X-ray fluorescence analysis indicated that quantities of TiO_2 in the synthesized catalysts were close to calculated values (Table 1).

SEM photographs of AC, TiO_2 and some TiO_2/AC demonstrate that the original AC powder consists of fragments of carbonized matter (Fig. 4A). The synthesized TiO_2 particles have spherical shape. Small TiO_2 particles with sizes in the range from 3 to 8 μm form large agglomerates with average size about 50–200 μm (Fig. 4B).

SEM photos illustrate that TiO_2 deposition by thermal hydrolysis of $TiOSO_4$ solution leads to formation of 3–5 μm size crystallites on the AC external surface (Fig. 4C) which becomes completely covered with TiO_2 particles as the TiO_2 content reaches 80 wt.% value (Fig. 4D).

XRD patterns of TiO_2 and some TiO_2/AC samples (Fig. 5) demonstrate that pure and deposited TiO_2 have only anatase modification. Rutile phase was not observed. It is typically for TiO_2 preparation by $TiOSO_4$ thermal hydrolysis [35]. The size of TiO_2 crystallites remains approximately constant in the s-TiO_2 and 80-, 70-TC samples and is equal to about 6 nm. It indicates that TiO_2 deposited on the AC surface in the case of high TiO_2 content is the same as s-TiO_2 sample, and it should not be expected change of TiO_2 itself spectral characteristics.

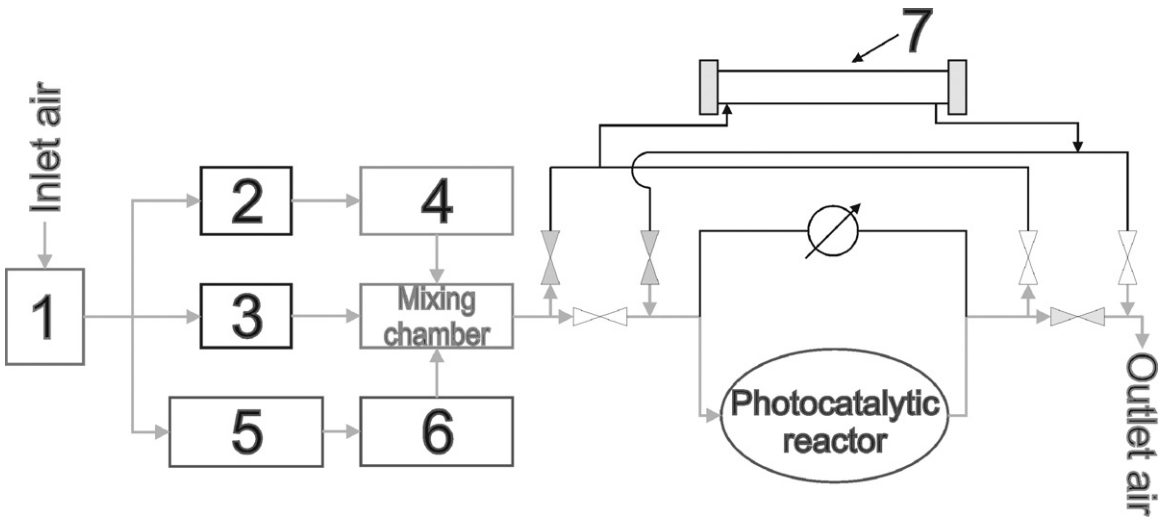

Fig. 3. Flow-circulating setup: (1) – air purification system; (2)–(3) – mass flow controllers, (4) – saturator with distilled water, (5) – saturator with cyclohexane, (6) – microdispenser, (7) – gas cell installed in an IR spectrometer.

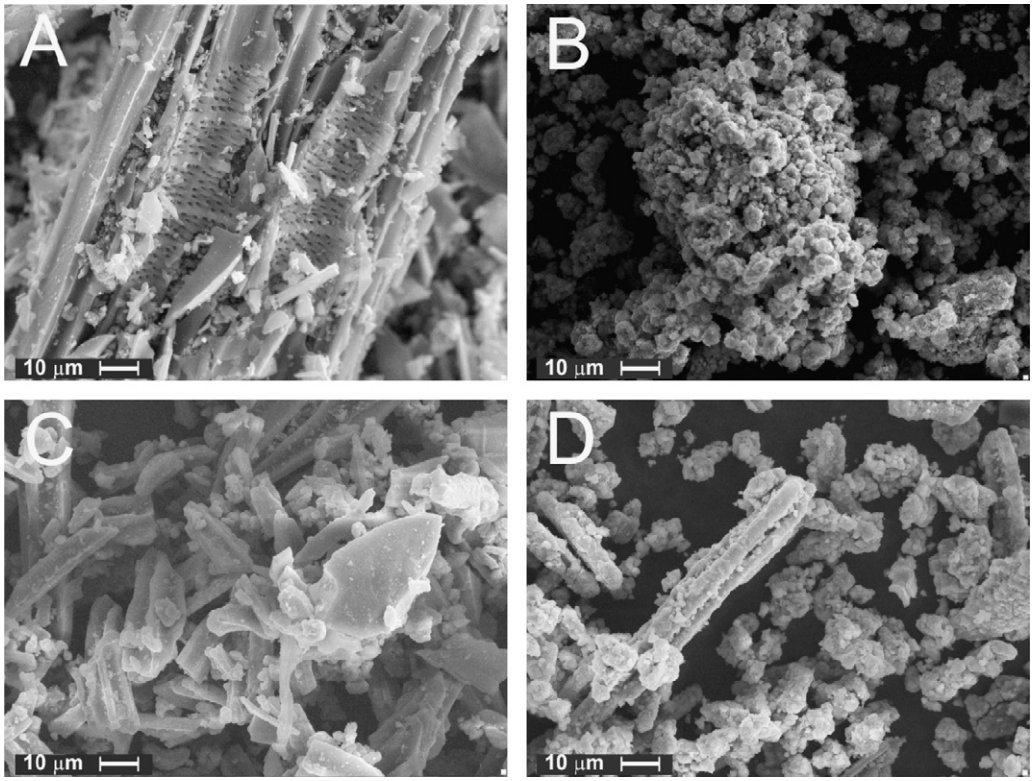

Fig. 4. SEM photographs of activated carbon (A), s-TiO_2 (B), 50-TC (C) and 80-TC (D) samples.

According to N_2 isotherms analysis (Table 1) the s-TiO_2 sample has large specific surface area S_{BET} = 167 m^2/g and pore volume V = 0.20 cm^3/g. The AC specific surface area is equal 825 m^2/g whereas micropore surface area calculated by *t*-plot analysis is equal 614 m^2/g. It means that AC structure mainly consists of micropores. Specific surface areas and pore volume of TC series samples are a superposition of the TiO_2 and AC individual characteristics (Fig. 6).

In visible region ($\lambda > 400$ nm) reflection intensity for TC series is lower than for the pure s-TiO_2 sample (Fig. 7). The reason of such behavior is light absorption by AC particles, which are not completely covered with TiO_2, because AC absorbs light both in visible and UV regions. Probably, it is one of the reasons of reducing oxidation rates for these composite catalysts as it will be demonstrated later.

Results of the physical–chemical analyses indicate that there does not occur considerable blocking of AC surface with supported TiO_2 particles and there is no difference between the pure synthesized TiO_2 powder and TiO_2 particles supported on the AC surface because TC series properties are a sum of s-TiO_2 and AC properties.

3.2. Photocatalytic oxidation experiments

3.2.1. Acetone vapor oxidation in the static reactor

In the beginning all synthesized samples were tested in the PCO of acetone vapor in the static reactor to choose the most active

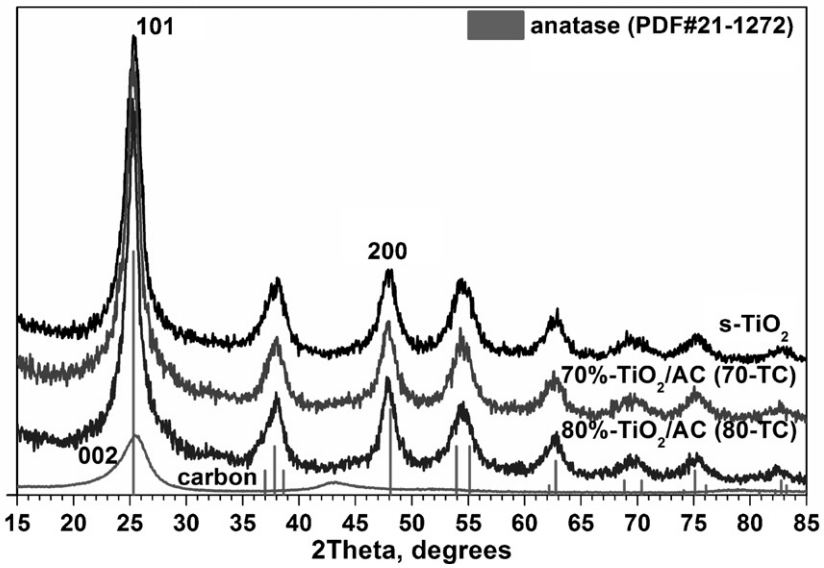

Fig. 5. XRD patterns of s-TiO_2, 80- and 70-TC samples.

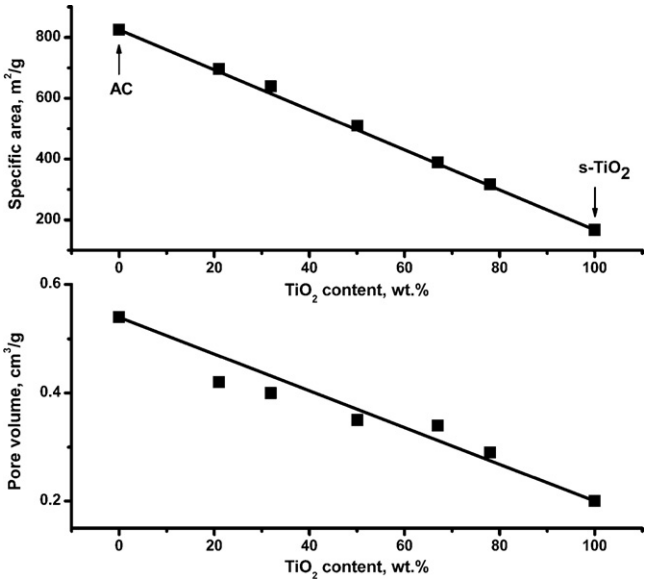

Fig. 6. Dependencies of specific surface area and pore volume on the TiO_2 content for TC series.

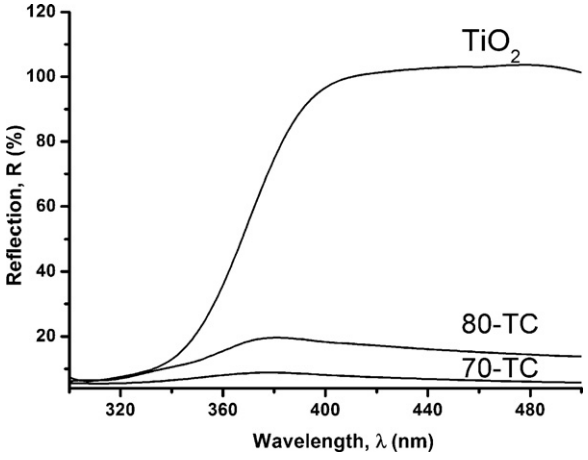

Fig. 7. Pure TiO_2 and TiO_2/AC diffuse reflectance spectra.

Table 2
Reaction parameters of acetone vapor PCO in the static reactor.

Sample	$\Delta C/C_0$ (%)[a]	W_{Ac} (ppm/min)	W_{CO_2} (ppm/min)
s-TiO_2	60	3.8	28
80-TC	68	3.0	22
70-TC	71	2.9	23
50-TC	77	1.2	10
30-TC	78	1.1	9
20-TC	80	0.9	6

[a] Amount of acetone adsorbed on the sample after establishment of adsorption–desorption equilibrium.

samples. Only water, carbon dioxide and CO were detected as products of oxidation. Amount of formed CO was about 15–30 ppm and was much lower than the final amount of evolved $CO_2 \sim 1250$ ppm so we did not take it into account in mass-balance.

The experimental data of acetone vapor removal and CO_2 accumulation during acetone photooxidation on the TC series and s-TiO_2 sample are presented in Fig. 8.

It could be seen that for s-TiO_2, 80- and 70-TC samples CO_2 concentration reached constant value after 60 min of irradiation (Fig. 8) and this value was slightly less than 100% of acetone conversion level. The rest carbon was in forms of gaseous CO and carbonates adsorbed on the catalyst surface. Samples with 20, 30 and 50 wt.% TiO_2 content demonstrated low oxidation rates therefore PCO reactions for these samples were not completed.

Table 2 summarizes the initial rates of acetone removal (W_{Ac}) and CO_2 accumulation (W_{CO_2}) calculated by linear approximation of experimental data for the first 40 min of PCO reaction. Amount of acetone adsorbed on the catalyst surface after establishment of the adsorption–desorption equilibrium ($\Delta C/C_0$) increased with increasing AC content in the sample. At the same time the rates of acetone removal (W_{Ac}) and CO_2 accumulation (W_{CO_2}) became less. In the other words the higher AC content corresponded to higher adsorption capacity and lower photocatalytic activity.

Acetone is a polar substance, probably that is a reason of the negative influence of AC content in composite photocatalyst on the kinetics of acetone vapor removal. So the next experiments were conducted with cyclohexane which adsorptivity on the AC surface has to be higher than for acetone.

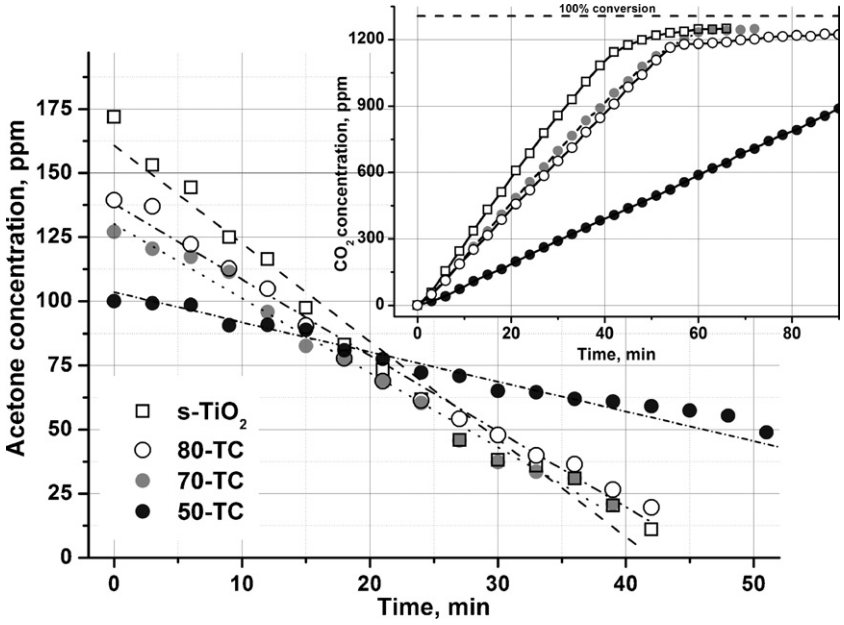

Fig. 8. Acetone vapor PCO in the static reactor with TC1 series photocatalysts and s-TiO_2.

3.2.2. Cyclohexane vapor oxidation

Cyclohexane vapor PCO on the composite TiO_2/AC photocatalysts was investigated in the static and flow reactors. The purpose of experiments in the static reactor was to understand the influence of AC presence on the reaction kinetics whereas flow reactor was used for measuring rate and adsorption constants.

3.2.2.1. Kinetics in the static reactor. Water, CO_2 and CO were detected as products of cyclohexane PCO. Final concentration of evolved CO in the static reactor was about 60–80 ppm whereas the final CO_2 concentration was about 3500 ppm that is why CO formation was neglected in mass-balance like in previous case.

Kinetic curves of C_6H_{12} removal and CO_2 accumulation are shown in Fig. 9 for s-TiO_2, 70-TC samples and for control experiment. The reason of control experiment was to understand difference between supported TiO_2/AC and spaced TiO_2 + AC cases. This control experiment will be described in detail later.

Starting C_6H_{12} concentration had to be C_0 = 603 ppm if to neglect adsorption. In the case of s-TiO_2 sample this starting concentration was decreased by ΔC = 39 ppm so that $\Delta C/C_0 \sim 6.5\%$ whereas in the case of composite photocatalysts the initial concentration drop was about $\Delta C \sim 210$ ppm, $\Delta C/C_0 \sim 35\%$ (Table 3). It means that TiO_2 has lower adsorption capacity in relation to nonpolar substrate – cyclohexane. The composite TiO_2/AC catalysts demonstrated substrate adsorption increased and its concentration in the gas phase was lower during the initial time period of photocatalytic reaction for 70-TC sample than for s-TiO_2 sample. However it should be noted that that there exists a cross-point time $t_s \sim 39.2$ min when gaseous cyclohexane concentration become higher for 70-TC than for s-TiO_2 samples. In other words the PCO rate becomes lower with TiO_2/AC photocatalyst.

Important characteristic of photocatalytic process is the time of maximum contaminant level (MCL) establishment (t_{MCL}) in static conditions. According to Russian sanitary regulations the cyclohexane MCL for working areas is 80 mg/m^3 which corresponds to 24 ppm concentration. The prolongation of cyclohexane removal kinetics for 70-TC photocatalysts and the increase of t_{MCL} time from 55 to 60 min also indicate that 70-TC sample is less efficient.

Activated carbon filters are often used in combination with photocatalytic filters in commercial air cleaning devices to decrease concentration of pollutants by adsorption. It was interesting to compare this way of adsorbent usage with the case of deposited TiO_2/AC photocatalyst. Therefore we carried out a control experiment, in which 4.8 mg of s-TiO_2 and 2.2 mg of AC powders were placed separately in the static reactor. TiO_2 and AC were taken in the same amounts as it was in the 7 mg of 70-TC sample.

Kinetics curves of cyclohexane removal and CO_2 accumulation during the control experiment are presented in Fig. 9 along with the data for s-TiO_2 and 70-TC samples. A significant decrease of the initial substrate concentration was observed: $\Delta C \sim 296$ ppm $\Delta C/C_0 \sim 49\%$. This value is even higher than for 70-TC sample although BET analysis demonstrated that specific surface area of 70-TC is equal to the algebraic sum of AC and s-TiO_2 surface areas (Fig. 6). To our opinion the explanation is that N_2 is a small molecule and the entire surface of 70-TC sample is available for it whereas cyclohexane molecule is bigger and a part of 70-TC sample surface is inaccessible due to partial blocking of AC with TiO_2 particles.

In control experiment cyclohexane concentration in gas phase was lowest during the initial time period of the PCO and maximum contaminant level was reached rapidly – t_{MCL} = 51.8 min (Table 3). On the other hand there was also observed a cross-point time t'_s = 57.6 min. After that time cyclohexane concentration in the control experiment became higher than in the case of s-TiO_2 sample and decreased very slowly. After 80 min of PCO for a long time period a trace level of cyclohexane vapor (about 3–7 ppm) was detected, whereas in case of s-TiO_2 or 70-TC samples it was removed from gas phase completely after 90 min of the PCO. It is the first difference between composite TiO_2/AC photocatalyst and simple combination of TiO_2 and AC.

The second observed difference could be seen from kinetic curves of CO_2 formation. In the control experiment (Fig. 9) the initial rate of CO_2 formation (W_{CO_2}) was 57 ppm/min but after 30 min of the PCO CO_2 formation rate decreased rapidly. Even after 4 h of the cyclohexane PCO carbon dioxide concentration in the static reactor reached only 3070 ppm level which corresponded to 85% mineralization ratio. It indicates that even after 4 h part of cyclohexane was remained adsorbed on the AC surface. In the case of 70-TC sample expected CO_2 level was almost achieved after 120 min of the PCO.

It is to be noted that total decrease of photocatalytic activity in case of composite catalyst or the separate use of TiO_2 and AC could

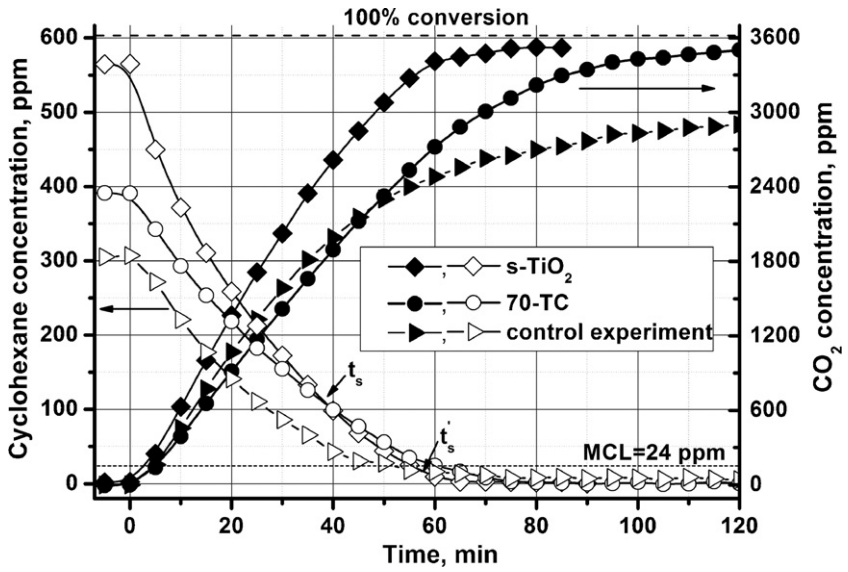

Fig. 9. Kinetics of C_6H_{12} PCO (unfilled markers) and CO_2 accumulation (filled markers) in the static reactor for s-TiO_2, 70-TC samples and control experiment.

Table 3
Characteristics of cyclohexane PCO kinetic curves presented in Fig. 9.

Sample	$\Delta C/C_0$ [a] (%)	t_s [b] (min)	t_{MCL} [c] (min)	W_{CO_2} [d] (ppm/min)
s-TiO_2	6.3	–	55.4	68
70-TC	35.2	39.2	60.4	50
Control experiment (4.8 mg s-TiO_2 + 2.2 mg AC)	49	57.6	51.8	57 (for the first 30 min)

[a] The amount of acetone adsorbed on the sample after establishment of adsorption–desorption equilibrium.
[b] The cross-point time of cyclohexane kinetic curves for TiO_2 and 70TC or TiO_2 + AC photocatalysts.
[c] The time of maximum contaminant level establishment; the MCL for cyclohexane is 24 ppm.[d]The initial rate of CO_2 formation for the first 40 min of the PCO.

be explained by the decrease of effective gaseous substrate concentration due to its adsorption on AC surface. This phenomenon has been previously studied by computer simulation of the PCO using L.-H. model [17]. But why is there exists different behaviors of 70-TC and separate TiO_2–AC systems? When TiO_2 and AC are used separately then substrate could transfer from adsorbent onto the TiO_2 surface only through gas phase and in the case of composite TiO_2/AC photocatalysts in addition there could occur a surface migration of substrate and intermediates. For example, cyclohexanone, carbonyl and carboxyl compounds [36] were detected as intermediates of the cyclohexane PCO. Thereby the separate use of photocatalyst and adsorbent results in considerable prolongation of substrate removal.

Experiments described above demonstrate that adsorption of oxidizing substrate strongly influence the kinetics of PCO in static conditions. Therefore to exclude this influence and determine the activity of TC samples experiments were carried out in flow conditions.

3.2.2.2. Kinetics in the flow reactor. Dependencies of cyclohexane steady-state PCO rate on its concentration for s-TiO_2, 80-TC and 70-TC samples in the flow reactor are presented in Fig. 10. Rate of CO_2 formation was taken as the rate of the PCO. Effective rate and adsorption constants were of interest in these steady-state experiments. L.-H. kinetic model was used to calculate them. This model corresponds to the following rate equation:

$$W_{CO_2} = \frac{k_r \cdot K_{ads} \cdot C}{1 + K_{ads} \cdot C},$$

where (W_{CO_2}) is the rate of CO_2, (k_r) is effective rate constant, (K_{ads}) is effective adsorption constant, (C) is the steady-state concentration of cyclohexane.

Experimental data for 70-TC and 80-TC as well as for unmodified TiO_2 were good approximated by the L.-H. equation. Resulting approximation curves are shown in Fig. 10 by dashed lines. Values of calculated effective rate and adsorption constants are presented in Table 4.

According to presented data TiO_2/AC samples revealed lower activity towards s-TiO_2 during cyclohexane oxidation in flow conditions if compare with experiments in the static reactor:

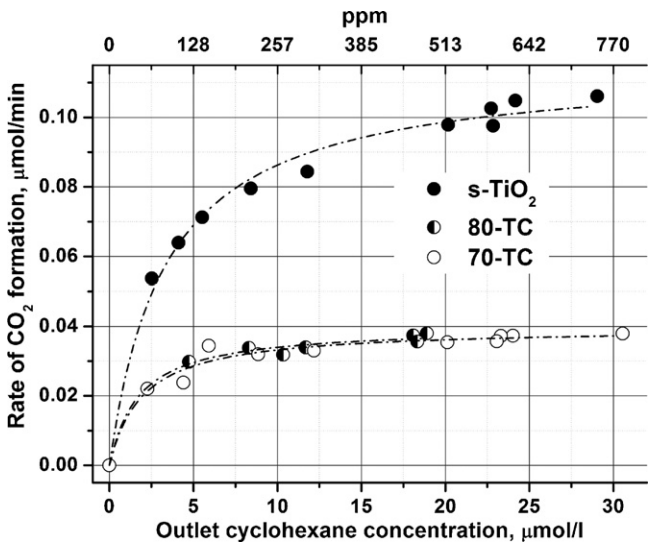

Fig. 10. Dependencies of cyclohexane steady-state oxidation rate on its concentration in the flow reactor. Dashed lines correspond to the approximation of experimental data by L.-H. equation.

Table 4
Results of cyclohexane kinetics approximation by L.-H. model.

Sample	Rate constant, k_r (μmol/min)	Adsorption constant, K_{ads} (l/μmol)	Product $k_r \cdot K_{ads}$
s-TiO_2	0.115 (±0.003)	0.3 (±0.03)	0.035
80-TC	0.040 (±0.002)	0.6 (±0.2)	0.024
70-TC	0.040 (±0.001)	0.5 (±0.1)	0.020

k_r = 0.040 μmol/min for 70-TC and 80-TC and 0.115 μmol/min for s-TiO_2. On the other hand the increase of adsorption constant (K_{ads}) was observed for the 70-TC and 80-TC composite photocatalysts. Probably during the formation of TiO_2 on the AC surface by thermal hydrolysis additional adsorption sites with higher absorptivity could form at TiO_2–AC interface.

Matos et al. [37] defined synergy factor (R) as:

$$R = \frac{k_{app(TiO_2+AC)}}{k_{app(TiO_2)}}$$

Cyclohexane kinetic curves from Fig. 9 could be used for estimation of R-factor in the first-order assumption. Apparent rate constant values for s-TiO_2, 70-TC and control experiment are equal to 0.044, 0.040 and 0.048 min^{-1} respectively. The corresponding R-factor values are:

$$R_1 = \frac{k_{app(70-TC)}}{k_{app(s-TiO_2)}} = 0.91 \quad \text{and} \quad R_2 = \frac{k_{app(control\ exp.)}}{k_{app(s-TiO_2)}} = 1.2.$$

Although control experiment revealed that C_6H_{12} traces remains for a very long time the calculated synergy effect was $R_2 > 1$. R-factor for composite sample (R_1) was close to 1. However if we will use L.-H. rate constant for product formation in steady sate experiments as activity criteria of the samples then this value will be lower: $R_1^{flow} = (0.040/0.115) = 0.35$ (Table 4). This short example supports the statement that correct R-factor has to be calculated only from product formation kinetic curves.

In our work we have managed to increase adsorption constant for composite TiO_2/AC system as compared with unmodified TiO_2. To our opinion lower value of rate constants is explained by lesser quanta quantity absorbed by AC particles incompletely covered with TiO_2.

3.3. Suggestion about structure of photocatalytically active TiO_2/AC catalysts with improved adsorption properties

Activated carbons still remain the most widely used adsorbents for air and water purification since this material has unique morphological properties which provide its high adsorption capacity against many types of organic molecule. But there exists certain difficulties of its wide application as a support for TiO_2 to prepare composite photocatalysts [29]. The main drawback is the UV light absorbance by AC particles. As it was demonstrated in the present work, all positive effects of AC are diminished by decrease of the oxidation rate due to lesser amount of light quanta absorbed by supported TiO_2. To improve the situation we suggest to synthesize composite systems based on specially structured or granulated activated carbon. External surface of such AC particles should be entirely covered with porous TiO_2 film. It is necessary for complete UV light absorption just by supported TiO_2. Therefore its thickness should be no less than 1 μm or about 2–3 wave lengths of absorbing light. If thickness of TiO_2 film would be less that a part of incident light will pass through this film and will be absorbed by AC. It is also necessary that internal surface of AC (surface of mesopores and micropores) would be unoccupied and unblocked by supported TiO_2 particles in order to enlarge adsorption of organic substrate to be oxidized. Proposed model is schematically shown in Fig. 11. In our opinion such structure of composite photocatalyst particles would be avoided of decreasing rates of photoreaction and would be able to improve the adsorption properties of photocatalysts.

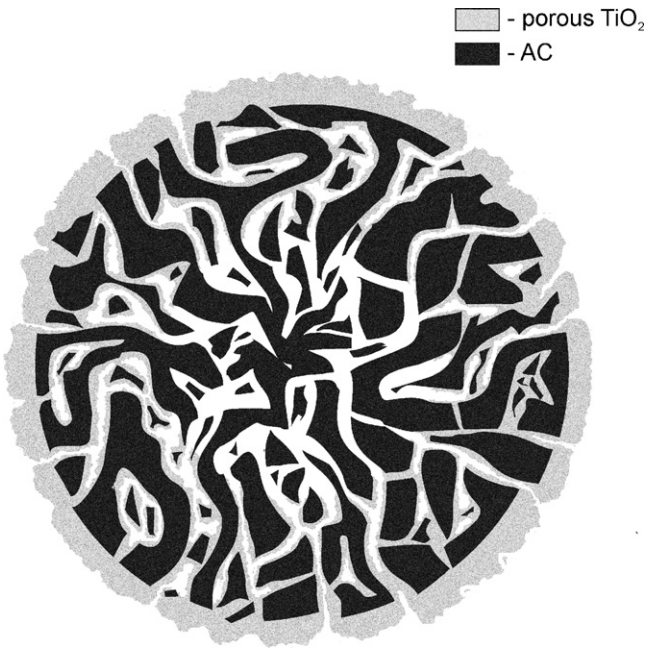

Fig. 11. Model of TiO_2/AC composite photocatalyst with increased photocatalytic and adsorption properties.

4. Conclusions

In the present work a synthesis of photocatalytically active composite TiO_2/AC catalysts with TiO_2 in anatase form was carried out. Photocatalytic activity was investigated in the PCO of acetone and cyclohexane vapor in the static and flow reactors. Complete photocatalytic mineralization of both model pollutants was observed without forming gaseous intermediates. Increase of adsorption capacity was observed for TiO_2/AC catalysts. This effect was pronounced in the case of nonpolar substrate – cyclohexane.

The same amounts of TiO_2 were used for PCO of equal portions of cyclohexane in the static reactor but in the first case this TiO_2 amount was deposited onto the AC and in the second case the same AC quantity was placed separately. A synergistic effect was observed and it was consisted in higher rate of CO_2 formation in the case of supported system whereas in the second case complete mineralization of cyclohexane was not achieved even after 4 h of the PCO. The most likely reason of such difference is the reversible surface transfer of reagents and intermediates between TiO_2 and AC surfaces. Such surface transfer was eliminated when TiO_2 and AC were used separately.

Approximation of steady-state kinetic data with the L.-H. model demonstrated that effective adsorption constants for TiO_2/AC photocatalysts became about 2 times higher than for pure TiO_2 during cyclohexane PCO.

To our opinion composite TiO_2/AC particles, which will demonstrate increase of both characteristics – adsorption capacity and mineralization activity – should be constructed of AC granules with available internal surface (micro- and mesopores) covered with porous TiO_2 layer. The thickness of this TiO_2 layer should be no less than 1–2 μm to absorb UV light completely.

Acknowledgements

We gratefully acknowledge the support of the Federal Special Program “Scientific and Educational Cadres of Innovative Russia”

(2009–2013 years) via contract P1360, SB RAS Integration projects 70 and 36, Presidium RAS grant 27.56 as well as the Ministry of Education and Science of Russia via contract 16.513.11.3091.

One of the authors (D.S.) appreciates the grant program "U.M.N.I.K." of "The Fund of Assistance to Development Small Forms of the Enterprises in Scientific and Technical Sphere".

References

[1] D.R.U. Knappe, Chapter 9: Surface chemistry effects in activated carbon adsorption of industrial pollutants, in: G. Newcombe, D. Dixon (Eds.), Interface Science and Technology, vol. 10, 2006, pp. 155–177.
[2] D.F. Ollis, H. Al-Ekabi (Eds.), Photocatalytic Purification and Treatment of Water and Air, Elsevier, 1993.
[3] M. Kaneko, I. Okura (Eds.), Photocatalysis: Science and Technology, Springer, 2002.
[4] A.L. Linsebigler, G. Lu, J.T. Yates, Chem. Rev. 95 (1995) 735–758.
[5] O. Carp, C.L. Huisman, A. Reller, Prog. Solid State Chem. 32 (2004) 33–177.
[6] A. Fujishima, T.N. Rao, D.A. Tryk, J. Photochem. Photobiol. C 1 (2000) 1–21.
[7] H. Einaga, S. Futamura, T. Ibusuki, Appl. Catal. B 38 (2002) 215–225.
[8] P.A. Kolinko, D.V. Kozlov, A.V. Vorontsov, S.V. Preis, Catal. Today 122 (2007) 178–185.
[9] K.Y. Foo, B.H. Hameed, Adv. Colloid Interface Sci. 159 (2010) 130–143.
[10] M.D. Hernández-Alonso, I. Tejedor-Tejedor, J.M. Coronado, M.A. Anderson, Appl. Catal. B 101 (2011) 283–293.
[11] D.V. Kozlov, A.V. Vorontsov, P.G. Smirniotis, E.N. Savinov, Appl. Catal. B 42 (2003) 77–87.
[12] H.-H. Ou, S.-L. Lo, J. Hazard. Mater. 146 (2007) 302–308.
[13] D.V. Kozlov, A.V. Vorontsov, J. Catal. 258 (2008) 87–94.
[14] W.-K. Jo, Ch.-H. Yang, Sep. Purif. Technol. 66 (2009) 438–442.
[15] F. Shiraishi, S. Yamaguchi, Y. Ohbuchi, Chem. Eng. Sci. 58 (2003) 929–934.
[16] J. Matos, J. Laine, J.-M. Herrmann, D. Uzcategui, J.L. Brito, Appl. Catal. B 70 (2007) 461–469.
[17] D.S. Selishchev, P.A. Kolinko, D.V. Kozlov, Appl. Catal. A 377 (2010) 140–149.
[18] P. Pucher, M. Benmami, R. Azouani, G. Krammer, K. Chhor, J.-F. Bocquet, A.V. Kanaev, Appl. Catal. A 332 (2007) 297–303.
[19] B. Herbig, P. Löbmann, J. Photochem. Photobiol. A 163 (2004) 359–365.
[20] Q. Zhang, J. Liu, W. Wang, L. Jian, Catal. Commun. 7 (2006) 685–688.
[21] X. Zhang, M. Zhou, L. Lei, Appl. Catal. A 282 (2005) 285–293.
[22] T. Torimoto, S. Ito, S. Kuwabata, H. Yoneyama, Environ. Sci. Technol. 30 (1996) 1275–1281.
[23] N. Takeda, T. Torimoto, S. Sampath, S. Kuwabata, H. Yoneyama, J. Phys. Chem. 99 (1995) 9986–9991.
[24] T. Guo, Z. Bai, C. Wu, T. Zhu, Appl. Catal. B 79 (2008) 171–178.
[25] B. Tryba, A.W. Morawski, M. Inagaki, Appl. Catal. B 41 (2003) 427–433.
[26] S.X. Liu, X.Y. Chen, X. Chen, J. Hazard. Mater. 143 (2007) 257–263.
[27] X. Zhang, L. Lei, J. Hazard. Mater. 153 (2008) 827–833.
[28] G.L. Puma, A. Bono, D. Krishnaiah, J.G. Collin, J. Hazard. Mater. 157 (2008) 209–219.
[29] R. Leary, A. Westwood, Carbon 49 (2011) 741–772.
[30] R. Yuan, R. Guan, J. Zheng, Scr. Mater. 52 (2005) 1329–1334.
[31] H.P. Kuo, C.T. Wu, R.C. Hsu, Powder Technol. 195 (2009) 50–56.
[32] C.H. Ao, S.C. Lee, Chem. Eng. Sci. 60 (2005) 103–109.
[33] N. Bouazza, M.A. Lillo-Rodenas, A. Linares-Solano, Appl. Catal. B 84 (2008) 691–698.
[34] T. Torimoto, Y. Okawa, N. Takeda, H. Yoneyama, J. Photochem. Photobiol. A 103 (1997) 153–157.
[35] D.M. Bavykin, V.P. Dubovitskaya, A.V. Vorontsov, V.N. Parmon, Res. Chem. Intermed. 33 (2007) 449–464.
[36] A.R. Almeida, J.A. Moulijn, G. Mul, J. Phys. Chem. C 115 (2011) 1330–1338.
[37] J. Matos, J. Laine, J.-M. Herrmann, Carbon 37 (1999) 1870–1872.